Oxidative Methane Coupling

DOI: 10.1002/anie.200802608

Rate and Selectivity Enhancements Mediated by OH Radicals in the Oxidative Coupling of Methane Catalyzed by $Mn/Na_2WO_4/SiO_2$**

*Kazuhiro Takanabe and Enrique Iglesia**

The oxidative coupling of methane (OCM) proceeds via complex primary and secondary pathways involving coupled heterogeneous and homogeneous reactions. These reactions form higher hydrocarbons, predominantly ethane and ethene, but also undesired CO_x.[1,2] Such pathways, which are described in Scheme 1, limit attainable C_2 yields[3–5] because

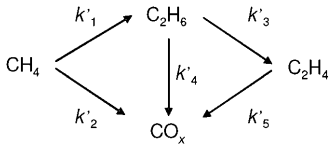

Scheme 1. Simplified scheme showing the OCM reaction network and pseudo-first-order rate constants for the respective steps.

of sequential reactions of C_2 products that are more reactive than CH_4[2] at the temperatures required to activate the C–H bonds in CH_4.[2] $Mn/Na_2WO_4/SiO_2$ catalysts are chosen here because of their high selectivity and stability during OCM reactions at such temperatures.[6–10]

Several studies have described homogeneous (gas-phase) and heterogeneous (surface-catalyzed) OCM reaction networks.[3–5,11,12] These networks capture most features of the measured rates and selectivities, but contain limited (or phenomenological) descriptions of the surface-mediated steps, often limited to C–H bond activation in CH_4, C_2H_6, and C_2H_4 using active oxygen species.[3–5,11,12] The remaining inconsistencies between measurements and models have been attributed to other surface-mediated pathways (e.g. quenching of unselective radicals, such as HOO•),[5,12] reversible CH_4 activation steps,[12] or to transport restrictions.[12]

Herein we report the marked effect of H_2O on OCM rates and selectivities caused by the catalytic generation of OH radicals, which react further to activate CH_4 in gas-phase reactions without net H_2O consumption. The high reactivity of these OH radicals weakens the sensitivity of H-abstraction rates on C–H bond energies, as suggested earlier.[13] The formation of OH radicals from O_2/H_2O mixtures on La_2O_3 and Nd_2O_3 materials that also catalyze OCM has been observed[14,15] and is proposed to influence OCM rates without concomitant effects on selectivity.[16] Two patents have described the effect of water on OCM rates and C_2 selectivities on MnO_x-based catalysts, although without mechanistic comment or interpretation.[17] Herein we rigorously describe the kinetic and mechanistic consequences of H_2O in OCM reactions and provide chemical and isotopic evidence for the involvement of OH radicals in H-abstraction and for the marked consequences of these pathways on attainable C_2 yields. We also comment more generally on the free-energy relations that cause more reactive H-abstractors to weaken the effects of C–H bond energies on reaction rates.

Figures 1a and 1b show differential CH_4 conversion rates as a function of contact time and C_{2+} selectivities as a function of CH_4 conversion, respectively, for $Mn/Na_2WO_4/SiO_2$ catalysts in gradient-less batch reactors. The CH_4 conversion rates increased with contact time and then decreased as O_2 was depleted in experiments where H_2O was neither added with the reactants nor removed as it formed ("steady state reaction"; Figure 1). The C_{2+} selectivities remained nearly constant up to around 10% CH_4 conversion but decreased at higher conversions (Figure 1b). These rate enhancements do not reflect the temperature gradients generally found for exothermic reactions in flow reactors,[10] which was ruled out by the lack of kinetic effects upon diluting the catalyst with inert solids (50:1). Recirculation minimizes transport effects by ensuring gradient-less operation and low CH_4 conversion per pass ($<1\%$).[18,19]

Rate enhancements with contact time may reflect the kinetic effects of products as they are formed, or of reactants as they are depleted, in gas-phase or surface reactions, or catalyst-structure and site-accessibility changes. Structural changes are inconsistent with the identical rates observed when the reaction mixtures were replaced with fresh CH_4/O_2 reactants. The kinetic effects responsible for rate enhancements may, however, reflect a negative kinetic order in CH_4 or O_2 or a positive order in one or more products (C_2H_6, C_2H_4, CO_x, H_2O).

The CH_4 conversion rates, as measured by extrapolation to zero conversion in a flow-reactor, were found to be proportional to CH_4 pressure and the square root of the O_2 pressure; these data rule out reactant depletion as the cause of the observed rate enhancements and agree with previous reports.[9] These kinetic data are consistent with the kinetic relevance of CH_4 activation by dissociated oxygen atoms (O*), which are formed by quasi-equilibrated O_2 dissociation as shown in the elementary steps (1)–(5), where *, M, and $[O_2]$ denote sites, "third bodies" required to dissipate energy

[*] Dr. K. Takanabe, Prof. E. Iglesia
Department of Chemical Engineering
University of California at Berkeley
Berkeley, CA 94720 (USA)
Fax: (+1) 510-642-4778
E-mail: iglesia@berkeley.edu
Homepage: http://iglesia.cchem.berkeley.edu/

[**] This study was supported by BP as part of the Methane Conversion Cooperative Research Program at the University of California at Berkeley.

Supporting information for this article is available on the WWW under http://dx.doi.org/10.1002/anie.200802608.

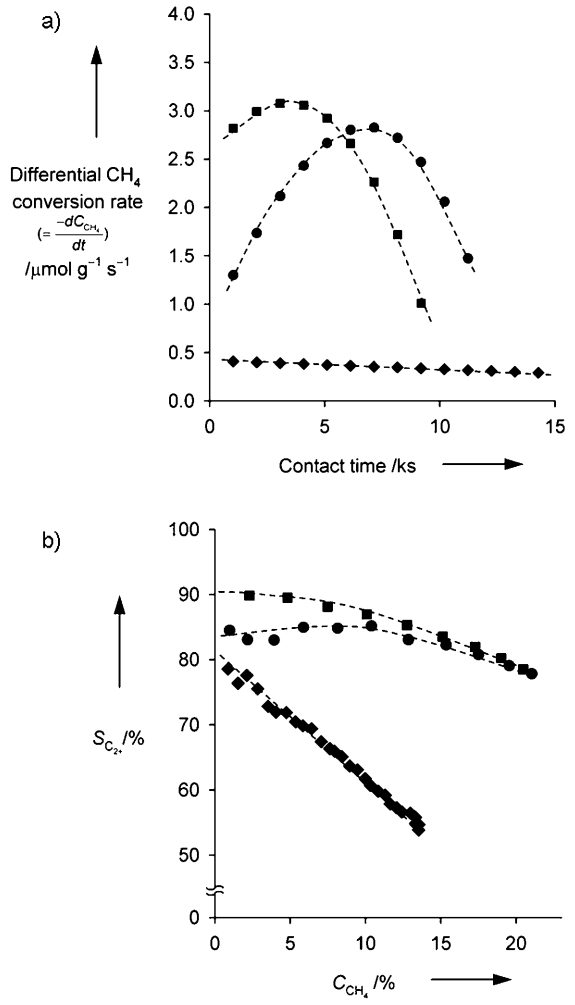

Figure 1. Plots of differential CH_4 conversion rate vs. contact time (a) and C_{2+} selectivity vs. CH_4 conversion (b); *S*: selectivity, *C*: conversion. ◆: H_2O removed; ●: steady state reaction; ■: H_2O added (0.02 g, 1073 K, unit volume: 275–650 mL, 10.7 kPa CH_4, CH_4/O_2 6:1, 0.4 kPa H_2O (when added), 101 kPa total pressure, balance He).

$$O_2 + 2* \overset{K_{O_2}}{\rightleftharpoons} 2\,O_s*;\ \rightleftharpoons \text{ denotes quasi-equilibrium} \quad (1)$$

$$CH_4 + O_s* \xrightarrow{k_{CH_4}} CH_3^{\bullet} + OH* \quad (2)$$

$$2\,OH* \rightleftharpoons H_2O + O* + * \quad (3)$$

$$2\,CH_3^{\bullet} + M \longrightarrow C_2H_6 + M \quad (4)$$

$$CH_3^{\bullet} + \alpha[O_2] \longrightarrow CO_x \quad (5)$$

during radical recombination, and active oxygen atoms involved in CO_x formation (which may differ from O*), respectively. The CH_4 conversion rates are given by Equation (6) at low O* coverages, which is consistent with the measured rates.

The C_2 products may cause rates to increase with increasing conversion by initiating homogeneous chain

$$r_{CH_4} = k' P_{CH_4} P_{O_2}^{1/2} \quad (6)$$

cycles, and $^{13}CH_4/O_2/^{12}C_2H_6$ or $^{13}CH_4/O_2/^{12}C_2H_4$ mixtures gave CH_4 conversion rate constants (k_1, k_2) identical to those without C_2H_6 or C_2H_4. Thus, C_2 products cannot account for the observed rate enhancements. $^{12}CH_4$ was not detected at any $^{13}CH_4$ conversion, which is consistent with the irreversible nature of the steps involving hydrocarbons in Scheme 1.

Water may influence OCM reactions via OH-mediated pathways produced by H_2O activation on oxide surfaces.[16] This proposal was tested by removing H_2O as it formed ("H_2O removed" in Figure 1) and by adding H_2O to CH_4/O_2 reactant mixtures ("H_2O added"). The removal of H_2O eliminated rate enhancements with conversion and led to rates that decreased with contact time because of depletion of CH_4 and O_2 (Figure 1 a). The C_2 selectivities decreased markedly as CH_4 conversion increased when H_2O was removed (Figure 1 b). In contrast, adding H_2O to CH_4/O_2 reactant mixtures increased initial conversion rates and C_2 selectivities markedly and weakened the effects of contact time on rates (Figures 1 a and 1 b).

H_2O/O_2 mixtures form OH radicals on La_2O_3-based OCM catalysts in a similar manner to $CH_3^{\bullet}$ radicals [step 2 above; Eq. (7)],[16] where $OH^{\bullet}$ and OH* denote radicals and chemisorbed species, respectively, and O_s* forms via step 1. The quasi-equilibria of steps 1, 3, and 7 mean that the equilibrium OH radical concentrations at 1173 K on La_2O_3 reflect the thermodynamics of the overall reaction [Eq. (8)].[15] We suggest here that H_2O increases OCM rates via OH-mediated homogeneous steps that abstract H-atoms from CH_4 [Eq. (9)].

$$H_2O + O_s* \rightleftharpoons OH^{\bullet} + OH* \quad (7)$$

$$O_2 + 2\,H_2O \overset{K_{OH^{\bullet}}}{\rightleftharpoons} 4\,OH^{\bullet} \quad (8)$$

$$CH_4 + OH^{\bullet} \xrightarrow{k'_{CH_4}} CH_3^{\bullet} + H_2O \quad (9)$$

The incremental rate (via step 9) using the OH radicals formed in step 8 is given by the second term in Equation (10)

$$r_{CH_4} = k' P_{CH_4} P_{O_2}^{1/2} + k'' P_{CH_4} P_{O_2}^{1/4} P_{H_2O}^{1/2} \quad (10)$$

with $k' = k_{CH_4} k_{O_2}^{1/2}$ and $k'' = k'_{CH_4} K_{O_2}^{1/4}$. Figure 2 shows the expected linear dependence on $P_{O_2}^{1/4} P_{H_2O}^{1/2}$ at short contact times (obtained from measured differences in rates with and without H_2O). The observed decrease in CH_4 conversion rate (Figure 2) reflects O_2 dissociation (step 1) steps that are no longer in equilibrium, as O_2 is depleted and H_2O concentration increases with increasing conversion. As a result, the rate of formation of O* decreases, and this species is scavenged more effectively by reactions with CH_4 via OH-mediated pathways that deplete O* to replenish OH as it reacts.

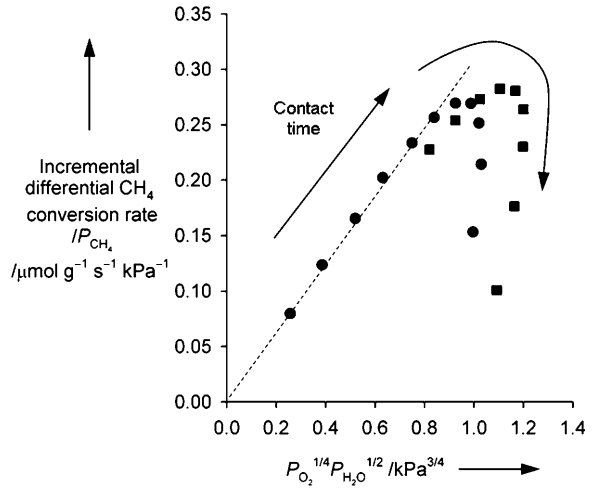

Figure 2. Plot of incremental differential CH_4 conversion rate (obtained from measured differences in rates with and without H_2O) vs. $P_{O_2}^{1/4} P_{H_2O}^{1/2}$. ●: steady state reaction; ■: H_2O added. The arrows indicate the increase in contact time (0.02 g, 1073 K, unit volume: 550–650 mL, 10.7 kPa CH_4, CH_4/O_2 6:1, 0.4 kPa H_2O (when added), 101 kPa total pressure, balance He).

Table 1: First-order rate constants (μmol g^{-1} s^{-1} kPa^{-1}) for the steps shown in Scheme 1 (0.02 g, 1073 K, 10.7 kPa $^{13}CH_4$, 1.7 kPa O_2, 0.4 kPa $^{12}C_2H_6/^{12}C_2H_4$, 0 or 0.4 kPa H_2O).

Rate constant	Surface-mediated	OH-mediated[a]
k'_1	0.05	0.16
k'_2 (k'_2/k'_1)	0.01 (0.25)	0.02 (0.11)
k'_3[b] (k'_3/k'_1)	1.7 (33)	1.1 (6.8)
k'_4[b] (k'_4/k'_1)	0.14 (2.7)	0.12 (0.73)
k'_5[c] (k'_5/k'_1)	0.22 (4.3)	0.10 (0.63)
$(k'_1+k'_2)/(k'_3+k'_4)$	0.03	0.14

[a] Calculated from rate differences with and without H_2O; [b] calculated from $^{13}CH_4/O_2/C_2H_6(/H_2O)$ mixtures; [c] calculated from $^{13}CH_4/O_2/C_2H_4(/H_2O)$ mixtures.

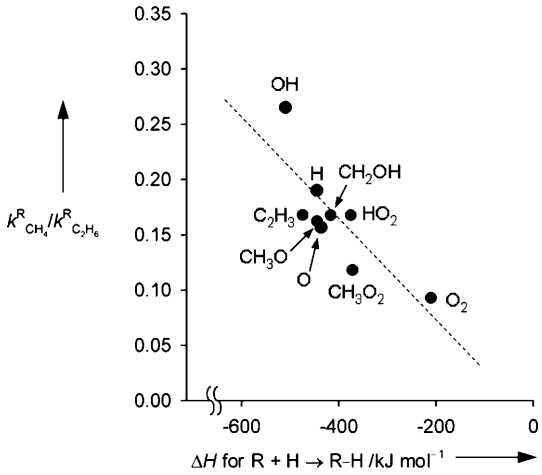

Figure 3. Ratios of rate constants $k^R_{CH_4}/k^R_{C_2H_6}$ for H-abstraction from CH_4 relative to C_2H_6 for various abstracting entities (R) vs. ΔH for the recombination reaction R + H → R–H at 1073 K.

The quasi-equilibrated nature of step 8 would lead to weak kinetic isotope effects (KIE) for $CH_4/O_2/H_2O$ and $CH_4/O_2/D_2O$ mixtures because OH activation precedes kinetically relevant steps. The measured H_2O/D_2O KIE value was 1.1. The CH_4/CD_4 KIE values for surface-catalyzed and homogeneous OH-mediated paths (steps 2 and 9) were found to be similar to each other and larger (1.3–1.4) than the H_2O/D_2O isotope effects, which is consistent with the involvement of C–H bonds in kinetically relevant steps and quasi-equilibrated formation of OH radicals via fast H_2O activation, even though the O–H bonds in H_2O (497 kJ mol^{-1}) are stronger than the C–H bonds in CH_4 (439 kJ mol^{-1}).[20] These trends reflect the stronger adsorption of H_2O than CH_4 on the vacant sites prevalent on oxides during OCM catalysis.

OH radicals, however, also activate C–H bonds in C_2H_6 and C_2H_4; yet, H_2O leads to higher C_2 selectivities (Figure 1b), apparently because OH radicals activate C–H bonds in C_2 molecules with less specificity (relative to CH_4) than oxide surfaces. $^{13}CH_4/O_2/C_2H_6$ and $^{13}CH_4/O_2/C_2H_4$ mixtures allowed accurate estimates for all rate constants in Scheme 1 (k'_1–k'_5) with and without H_2O to be obtained (Table 1). All rate constants were larger when H_2O was present, although those for CH_4 activation showed the largest increase. As a result of these OH-mediated activation pathways, the k'_i/k'_1 ratios decreased for all species, thus causing the observed increase in C_2 selectivities and yields with H_2O.

Figure 3 gives the rate constant ratios reported for H-abstraction from CH_4 and C_2H_6 ($k^R_{CH_4}/k^R_{C_2H_6}$) in homogeneous reactions with various abstractors (R).[5,21] This ratio increases as the RH products become more stable (R + H → R–H, more exothermic). These abstraction reactions become less sensitive ($k^R_{CH_4}/k^R_{C_2H_6}$ is larger) to differences in energy between the C–H bonds in CH_4 and C_2H_6 (CH_4: 439 kJ mol^{-1}; C_2H_6: 423 kJ mol^{-1})[20] as the abstraction products become more stable, as is also the case for the relative rates of HCHO and CH_4 oxidation via homogeneous pathways.[22] OH radicals lead to very exothermic H-abstraction reactions and to the highest $k^R_{CH_4}/k^R_{C_2H_6}$ ratios (Figure 3). Consistent with this, the involvement of OH radicals in H-abstraction increases the $\{(k'_1+k'_2)/(k'_3+k'_4)\}$ ratios markedly, from 0.03 for surface-mediated pathways to 0.14 for OH-mediated pathways (Table 1).

H_2O also leads to lower k'_5/k'_1 ratios (4.3 without H_2O; 0.63 for OH-mediated pathways; Table 1), which is consistent with the preferential enhancement of CH_4 over C_2H_4 activation rates by OH-mediated routes. Surfaces oxidize C_2H_4 (k'_5) more effectively than CH_4 (k'_2) or C_2H_6 (k'_4), in spite of the strong C–H bonds in C_2H_4 (463 kJ mol^{-1}),[20] apparently because C_2H_4 is strongly adsorbed.[23] OH-mediated pathways do not involve adsorption and lead to k'_5/k'_1 values below unity (0.63). These ratios faithfully reflect the stronger C–H bonds in C_2H_4, without compensation by adsorption energies. In fact, these previously unrecognized OH-mediated pathways are essential to achieving the maximum C_2 yields reported (up to 26%), which could not be reached with contributions from surface-mediated pathways only.

We have achieved C_{2+} yields of 26% by replenishing O_2 after it is depleted in order to avoid explosive reactant mixtures (Figure 4). These yields match the highest values

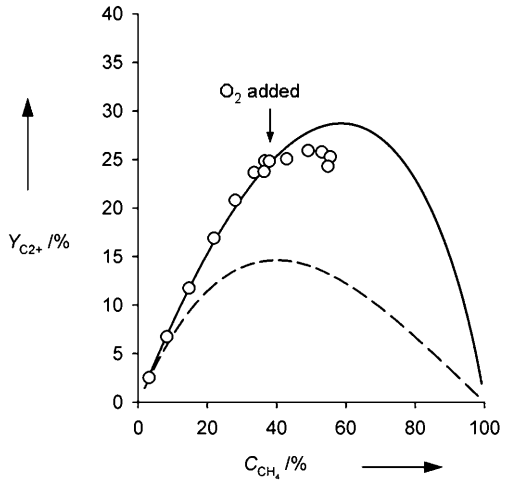

Figure 4. Plot of C_{2+} yield vs. CH_4 conversion for experimental data and pseudo-first-order kinetic models using the rate constants shown in Table 1. (0.02 g, 1073 K, unit volume: 550 mL, 4.0 kPa CH_4, 1.3 kPa O_2 (initial), 1.5 kPa O_2 (added) 101 kPa total pressure, balance He). -----: the "dry" model; ——: the "wet" model.

reported previously.[6] A kinetic model based on Scheme 1 and rate constants for surface- and OH-mediated pathways (Table 1; see the Supporting Information for further details) accurately describes the measured yields and predicts a maximum possible C_2 yield of 29%. Figure 4 shows that the rate constants for surface-mediated pathways, which prevail in the absence of H_2O, cannot account for observed C_2 yields and predict maximum values of only 15%.

In summary, this study provides mechanistic evidence that OH-mediated C–H bond activation pathways are essential for attaining practical yields and describing the evolution of C_2 yields during catalytic reactions. The ability of oxide catalysts to generate equilibrium OH-radical concentrations provides opportunities to exploit pathways mediated by such radicals in related chemistries. Our data provide compelling evidence for the benefits of using more reactive species (or higher temperatures) to weaken the sensitivity of H-abstraction reactions to C–H bond energies, a challenge and hurdle that limits the maximum attainable yields of the desired products in most practical applications of oxidation catalysis.[24]

Experimental Section

SiO_2 (Davison chemical, Silica Gel Grade 57) was impregnated with aqueous $Mn(NO_3)_2$ (50 wt.%, STREM Chemicals; 2 mL g^{-1} of SiO_2) and the mixture dried in ambient air at 403 K for 5 h.[8] This sample was then impregnated with an aqueous solution of $Na_2WO_4{\cdot}2H_2O$ (99%, Sigma–Aldrich, 2 mL g^{-1} of SiO_2) to give a sample containing 2 wt.% Mn and 5 wt.% Na_2WO_4. This sample was dried at 403 K for 5 h and then heated in flowing dry air (Praxair, UHP, 0.167 mL s^{-1}) at 1173 K (temperature increase: 0.033 K s^{-1}) for 8 h. The samples were sieved to retain 0.25–0.35-mm aggregates.

OCM rates and selectivities were measured in flow or recirculating batch reactors using a U-shaped quartz cell (4 mm I.D.).[18] Samples (0.02 g) were mixed with quartz powder (0.5 g; Fluka, SiO_2, 0.25–0.35 mm) and held onto quartz wool. The temperature was maintained with a Watlow controller (Series 982) coupled to a resistively heated furnace and measured with a type K thermocouple set outside the catalyst bed. CH_4 (Praxair, 99.999%) and O_2 (Praxair, 99.999%) were introduced with He (Praxair, 99.999%) as diluent. In batch experiments, the recirculation loop (275–650 mL) was evacuated to <0.1 Pa before introducing the reactants, which were circulated with a graphite gear micropump (>2.5 mL s^{-1}). H_2O was removed from the reactor loop using a dry ice/acetone trap, which does not condense other products. Reactant and product concentrations were measured with an HP5890 gas chromatograph using a Carbosieve SII packed column (Supelco, 3.2 mm × 2 m) with thermal conductivity detection and a HP-PLOT Q capillary column (Agilent, 0.32 mm × 30 m) with flame ionization detection. Differential rates were obtained from time-derivatives of CH_4 concentration profiles vs. time measured in batch reactors after regression to a polynomial fit. Selectivities are reported on a carbon basis as cumulative (integral) values.

CD_4 (Isotec, 99 atom%-D) and D_2O (Cambridge Isotope Laboratories, Inc., 99.9%) were used to measure kinetic isotope effects. Tracer studies used labeled $^{13}CH_4$ (Isotec, 99 atom%-^{13}C) in the presence of $^{12}C_2H_6$ (Praxair, 99.999%) or $^{12}C_2H_4$ (Praxair, 99.999%). These isotopic measurements were carried out in a batch recirculating reactor equipped with two HP5890 gas chromatographs, with combined thermal conductivity, flame ionization and mass selective detectors. The latter was connected to an HP-PLOT Q capillary column used for isotopic detection.

Received: June 4, 2008
Published online: September 2, 2008

Keywords: hydrogen abstraction · kinetics · oxidative coupling of methane · radical reactions · reaction mechanisms

[1] G. E. Keller, M. M. Bhasin, *J. Catal.* **1982**, *73*, 9–19.
[2] J. H. Lunsford, *Catal. Today* **2000**, *63*, 165–174.
[3] a) J. A. Labinger, K. C. Ott, *J. Phys. Chem.* **1987**, *91*, 2682–2684; b) J. A. Labinger, *Catal. Lett.* **1988**, *1*, 371–376.
[4] a) S. C. Reyes, E. Iglesia, C. P. Kelkar, *Chem. Eng. Sci.* **1993**, *48*, 2643–2661; b) S. C. Reyes, C. P. Kelkar, E. Iglesia, *Catal. Lett.* **1993**, *19*, 167–180.
[5] C. A. Mims, R. Mauti, A. M. Dean, K. D. Rose, *J. Phys. Chem.* **1994**, *98*, 13357–13372.
[6] A. Palermo, J. P. H. Vazquez, A. F. Lee, M. S. Tikhov, R. M. Lambert, *J. Catal.* **1998**, *177*, 259–266.
[7] X. Fang, S. Li, J. Lin, J. Gu, D. Yang, *J. Mol. Catal. (China)* **1992**, *6*, 427.
[8] D. Wang, M. P. Rosynek, J. H. Lunsford, *J. Catal.* **1995**, *155*, 390–402.
[9] S. Pak, P. Qiu, J. H. Lunsford, *J. Catal.* **1998**, *179*, 222–230.
[10] S. Pak, J. H. Lunsford, *Appl. Catal. A* **1998**, *168*, 131–137.
[11] A. J. Colussi, V. T. Amorebieta, *J. Catal.* **1997**, *169*, 301–306.
[12] Y. S. Su, J. Y. Ying, W. H. Green, *J. Catal.* **2003**, *218*, 321–333.
[13] J. A. Labinger, *J. Mol. Catal. A* **2004**, *220*, 27–35.
[14] L. C. Anderson, M. Xu, C. E. Mooney, M. P. Rosynek, J. H. Lunsford, *J. Am. Chem. Soc.* **1993**, *115*, 6322–6326.
[15] K. B. Hewett, L. C. Anderson, M. P. Rosynek, J. H. Lunsford, *J. Am. Chem. Soc.* **1996**, *118*, 6992–6997.
[16] K. B. Hewett, M. P. Rosynek, J. M. Lunsford, *Catal. Lett.* **1997**, *45*, 125–128.
[17] a) A. M. Gaffney, US Patent, 4788372, **1988**; b) D. W. Leyshon, US Patent, 4801762, **1989**.
[18] E. Iglesia, J. E. Baumgartner, G. L. Price, K. D. Rose, J. L. Robbins, *J. Catal.* **1990**, *125*, 95–111.

[19] J. A. Roos, S. J. Korf, R. H. J. Veehof, J. G. van Ommen, J. R. H. Ross, *Appl. Catal.* **1989**, *52*, 131 – 145.
[20] S. J. Blanksby, G. B. Ellison, *Acc. Chem. Res.* **2003**, *36*, 255 – 263.
[21] GRI-Mech v.3.0. G. P. Smith, D. M. Golden, M. Frenklach, N. W. Moriarty, B. Eiteneer, M. Goldenberg, C. T. Bowman, R. K. Hanson, S. Song, W. C. Gardiner, Jr., V. V. Lissianski, Z. Qin, http://www.me.berkeley.edu/gri_mech/.
[22] J. M. Zalc, W. H. Green, E. Iglesia, *Ind. Eng. Chem. Res.* **2006**, *45*, 2677 – 2688.
[23] J. A. Dumesic, D. F. Rudd, L. M. Aparicio, J. E. Rekoske, A. A. Treviño, *The Microkinetics of Heterogeneous Catalysis*, American Chemical Society, Washinton, DC, **1993**.
[24] a) C. Batiot, B. K. Hodnett, *Appl. Catal. A* **1996**, *137*, 179 – 191; b) A. Costine, B. K. Hodnett, *Appl. Catal. A* **2005**, *290*, 9 – 16.

